Journal of Power Sources 196 (2011) 4355–4363

Contents lists available at ScienceDirect

Journal of Power Sources

journal homepage: www.elsevier.com/locate/jpowsour

Preliminary analysis of compound systems based on high temperature fuel cell, gas turbine and Organic Rankine Cycle

D. Sánchez*, J.M. Muñoz de Escalona, B. Monje, R. Chacartegui, T. Sánchez

Escuela Técnica Superior de Ingenieros de Sevilla, Camino de los Descubrimientos s/n, 41092 Sevilla, Spain

ARTICLE INFO

Article history:
Received 1 June 2010
Received in revised form 16 July 2010
Accepted 23 July 2010
Available online 1 August 2010

Keywords:
MCFC
Compound
Organic
ORC

ABSTRACT

This article presents a novel proposal for complex hybrid systems comprising high temperature fuel cells and thermal engines. In this case, the system is composed by a molten carbonate fuel cell with cascaded hot air turbine and Organic Rankine Cycle (ORC), a layout that is based on subsequent waste heat recovery for additional power production. The work will credit that it is possible to achieve 60% efficiency even if the fuel cell operates at atmospheric pressure.

The first part of the analysis focuses on selecting the working fluid of the Organic Rankine Cycle. After a thermodynamic optimisation, toluene turns out to be the most efficient fluid in terms of cycle performance. However, it is also detected that the performance of the heat recovery vapour generator is equally important, what makes R245fa be the most interesting fluid due to its balanced thermal and HRVG efficiencies that yield the highest global bottoming cycle efficiency. When this fluid is employed in the compound system, conservative operating conditions permit achieving 60% global system efficiency, therefore accomplishing the initial objective set up in the work.

A simultaneous optimisation of gas turbine (pressure ratio) and ORC (live vapour pressure) is then presented, to check if the previous results are improved or if the fluid of choice must be replaced. Eventually, even if system performance improves for some fluids, it is concluded that (i) R245fa is the most efficient fluid and (ii) the operating conditions considered in the previous analysis are still valid.

The work concludes with an assessment about safety-related aspects of using hydrocarbons in the system. Flammability is studied, showing that R245fa is the most interesting fluid also in this regard due to its inert behaviour, as opposed to the other fluids under consideration all of which are highly flammable.

1. Introduction

Hybrid systems formed by high temperature fuel cells and bottoming gas turbines have been investigated thoroughly in the last decade, either theoretically [1,2] or experimentally [3,4], as a means to achieve higher efficiency and specific power. Early proposals were based on supercharging stand alone fuel cells, taking advantage of the favourable effect of higher operating pressures on cell performance and dismissing any potential contribution of the compressor/turbine coupling [5]. On the contrary, later developments concentrated on exploiting the gas turbine system which was no more conceived as a simple turbocharger but as an externally fired engine capable of providing additional power. Several works reported that a 10–20% extra power capacity could be expected depending on the type of fuel cell–turbine integration [6].

The development of hybrid systems has experienced different phases, ranging from the very optimistic initial steps, which envisaged attainable efficiencies higher than 70%, to more cautious predictions of around 55%. Also the type of fuel cell used has been subjected to discussion, giving priority to the very high operating temperature of solid oxide fuel cells or the higher maturity of molten carbonate technology. For both cases, there are, or have been, experimental plants in operation [4,7].

Broadly speaking, there seems to be consensus within the scientific and industrial communities that hybrid systems will have difficulties in breaking the 60% efficiency barrier, at least for first generation systems. The need to reduce the operating temperature of SOFCs to around 750 °C and the very moderate fuel utilization factors achieved by state of the art MCFCs are just two of the major hurdles that must be overcome if system efficiency is to be increased.

This work presents the fundamentals of an advance hybrid system where a combined bottoming cycle is employed in lieu of a conventional single gas turbine engine. Such system, for which the term compound has been adopted, comprises an ordinary

* Corresponding author. Tel.: +34 954 48 64 88; fax: +34 954 48 72 43.
E-mail address: davidsanchez@esi.us.es (D. Sánchez).

0378-7753/$ – see front matter © 2010 Elsevier B.V. All rights reserved.
doi:10.1016/j.jpowsour.2010.07.060

Nomenclature

A	active cell area (m^2)
BC	bottoming cycle
E	Nernst voltage (V)
F	Faraday constant
GT	gas turbine
h	mass enthalpy ($kJ\,kg^{-1}$)
h_m	molar enthalpy ($J\,mol^{-1}$)
HRVG	heat recovery vapour generator
j	current density ($A\,m^{-2}$)
K	equilibrium constant
$\dot{m}$	mass flow rate ($kg\,m^{-3}$)
M	molar mass ($g\,mol^{-1}$)
n	molar flow rate ($mol\,s^{-1}$)
MCFC	molten carbonate fuel cell
SOFC	solid oxide fuel cell
ORC	organic Rankine cycle
p	pressure (bar)
PR	pressure ratio
R	resistance ($\Omega\,m^2$)
T	temperature (K)
$\bar{T}$	mean temperature (K)
TIT	turbine inlet temperature (K)
U_{CO_2}	carbon utilization (%)
U_f	fuel utilization (%)
V	cell voltage (V)
W	specific/useful work ($kJ\,kg^{-1}$)
$\dot{W}_{el}$	electric power (W)
x	molar fraction

Greek symbols

η	efficiency
ρ	density ($kg\,m^{-3}$)

Subscripts

a	addition
c	rejection
cr	critical
ign	ignition
lim	limit
t	turbine
th	thermal
p	pump

high temperature fuel cell and gas turbine hybrid system that is complemented by an Organic Rankine Cycle ORC for additional heat recovery and power production. This surplus work allows a 5% efficiency increase with respect to the reference system, therefore surpassing the aforementioned crystal roof of efficiency set at 60%.

The work is divided in four different parts. First, the concept of compound system is exposed and its layout presented in a simplified sketch. Then, the effect on system performance of using different working fluids in the ORC subsystem is discussed. As shown later, optimum performances of ORC and compound system are not necessarily correlated in a direct simple way. Finally, system optimisation is carried out with respect to the most relevant operating parameters of the heat engines under consideration: gas turbine pressure ratio and ORC live steam pressure/temperature. Again, interesting results are obtained with respect to their respective weights on global efficiency. The work closes with some relevant considerations regarding safety operation of organic fluids.

Table 1
Carnot's equivalent efficiency.

	$\bar{T}_a$ (°C)	$\bar{T}_c$ (°C)	$\eta_{Carnot,\,eq}$ (%)
HTFC	600–900	600	–
GT_{rec}	450	150–250	28–41
ORC	200	35	35
HTFC + GT_{rec}	600–900	150–250	40–64
HTFC + GT_{rec} + ORC	600–900	35	64–74

2. Concept of compound system

The concept of compound hybrid system is better described by making use of a thermodynamic analysis based on Carnot's equivalence. Following this approach, the efficiency of a power cycle that absorbs and rejects heat at constant temperatures T_a and T_c respectively can be approximated by:

$$\eta_{Carnot,eq} = 1 - \frac{T_c}{T_a} = 1 - \frac{\bar{T}_c}{\bar{T}_a} \quad (1)$$

Strictly speaking, Eq. (1) is only applicable to cycles where heat absorption/rejection takes place at constant temperature and work is consumed/generated at constant entropy. Nevertheless, the concept of Carnot's equivalent efficiency as presented in Eq. (1) can be extended to any power cycle, despite the nature of their internal processes, just by defining representative mean temperatures for the heat exchange processes, $\bar{T}$ in Eq. (1). This simple approach enables an easier development of complex energy systems.

Table 1 shows representative values of $\bar{T}_a$ and $\bar{T}_c$ for high temperature fuel cells, recuperative gas turbines and Organic Rankine Cycles even though, in purity, fuel cells cannot be regarded as heat engines and the concept of Carnot's equivalent efficiency is therefore not applicable. Some interesting conclusions can be drawn from the information in Table 1:

- Fuel cells are very interesting for their high heat addition temperature.
- Organic Rankine Cycles are very interesting for their very low heat rejection temperature. These power systems are based on a biphasic power cycle where the working fluid is a hydrocarbon based compound, whether a pure fluid or a mixture [8–10]. More details about the cycle are given in Section 3.
- There is an important thermal gap between these two temperatures which would inevitably lead to high exergy losses when heat is transferred from topping to bottoming cycle.
- Gas turbines are likely to fill this thermal gap, approaching hot and cold temperatures of intermediate heat exchange processes while generating power and, therefore, increasing global efficiency. Gas turbines are based on the Brayton cycle which is a single phase open power cycle where fresh air is compressed, heated up and then expanded [11], Fig. 1. Heating the gas can be performed either by internal combustion or by an external heat source, as it is the case for hybrid systems.

Fig. 1 provides a simplified layout of a compound system formed by molten carbonate fuel cell, recuperative gas turbine and Organic Rankine Cycle as suggested by Table 1. Each subsystem is enclosed in a different box to illustrate the rather independent assembly that easily permits stand alone operation of the cell without the bottoming cycles. In this regard, two features of this proposal are worth being mentioned:

- There is minimum integration between subsystems: only one heat exchanger connects adjacent control volumes in Fig. 1. More complex integration between gas turbine exhaust gases and

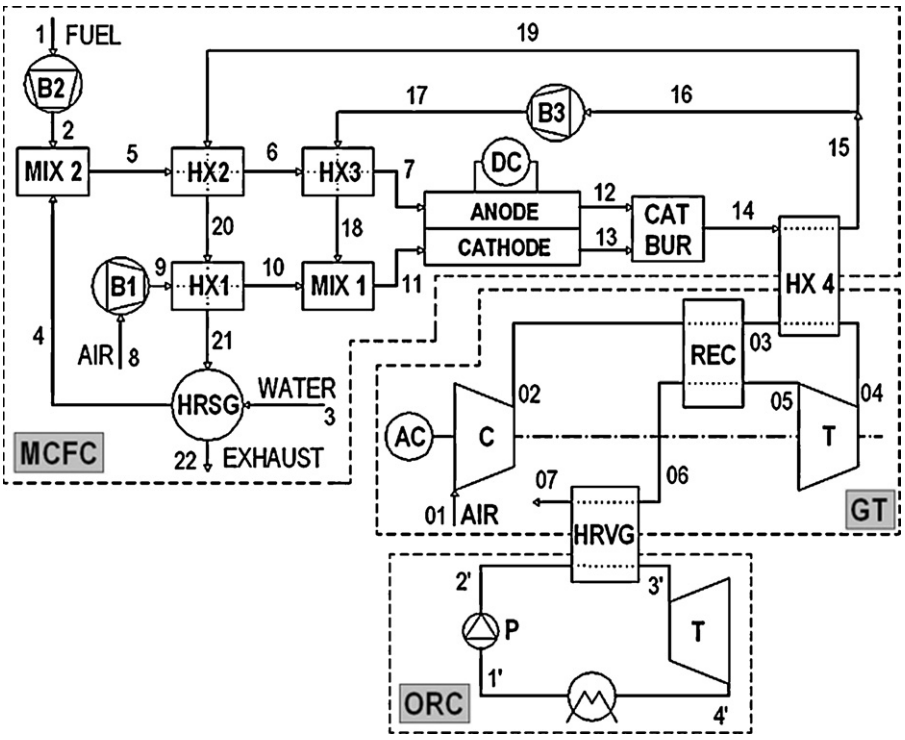

Fig. 1. Compound system layout.

Table 2
Typical exhaust temperature of recuperated Brayton cycles.

TIT (°C)	PR_{opt}	η_{GT} (%)	T_{06} (K)
600	5.5	30.5	573
700	6.6	33.5	606
800	7.8	36.2	637
900	9.0	38.6	668
1000	10.4	40.7	697

MCFC fuel/air preheating has been intendedly avoided.

- Following this concept, fuel cell pressurization has not been considered even though some existing systems [7] make use of the compressor to feed the cathode of the fuel cell directly, therefore benefiting from a higher operating pressure. In this case, atmospheric operation of the fuel cell has been preferred. Though this topic is out of the scope of this work, this is expected to yield longer useful life to the fuel cell stack.

Available temperatures at gas turbine exhaust depend on whether the unit is recuperated or not. Considering the recuperated case, exhaust temperatures (state 06 in Fig. 1) are estimated in the range from 573 to 673 K when turbine inlet temperature varies from 873 to 1273 K, which is representative of MCFC and SOFC technologies. These estimations are derived from a simplified thermodynamic analysis of recuperated engines working at their respective optimum pressure ratios PR_{opt} and typical internal efficiencies of compressor and turbine[1], Table 2.

[1] Saravanamuttoo et al. [11] show that there exist two different optimum pressure ratios for gas turbine engines: pressure ratio for maximum efficiency and pressure ratio for maximum useful work. For recuperated engines, maximum efficiency is achieved at a lower pressure ratio than maximum useful work while, for non-recuperated engines, the opposite is true. Within the scope of this work, optimum pressure ratio is always regarded as referred to maximum efficiency, even if this dualism does not affect the rough estimations given in Table 2.

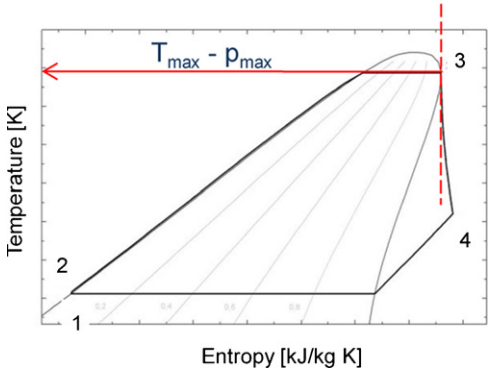

Fig. 2. Standard *T*–*s* diagram of reference ORC cycle.

Table 2 sets an upper limit for the ORC maximum temperature ($T_{3'}$ in Fig. 1) at around 600 K for MCFC based compound systems and 650 K if SOFCs are used. This constraint gives way to an optimisation process whose outcome must indicate which organic fluid provides better efficiency. Such process is shown in the following section.

3. ORC cycle analysis and selection of fluid

Rankine cycles comprise the following series of processes to convert heat into useful work, Fig. 2: liquid compression (1′-2′), vapourization (2′-3′), gaseous expansion (3′-4′) and condensation (4′-1′). Due to the phase change of the working fluid, there is a large difference in compressibility from compression to expansion that results in a very high useful to expansion work ratio.

Modern steam cycles achieve 50% thermal efficiency when very high live steam parameters and complex layouts are used. In this regard, Table 2 evidences that live steam temperatures higher than 575 K are not feasible if the proposed compound system is to be applied to MCFCs and, even for SOFCs, it is not possible to exceed

Table 3
Organic fluids under consideration.

	M (g mol^{-1})	T_{cr} (K)	P_{cr} (bar)	T_{max} (K)	P_{max} (bar)	T_{lim} (K)
Toluene	92.14	591.7	41.3	569	31.2	671.9
Cyclohexane	84.16	553.6	40.8	536	32.7	560.7
n-Hexane	86.18	507.9	30.6	491	26.6	–
Isopentane	72.15	460.4	33.7	448	27.9	–
R245fa	134	427.2	36.5	403	23.3	–
Isobutane	58	407.8	36.4	380	22.5	413.3

650 K. Additionally, since the ORC cycle in Fig. 1 is expected to generate a minor fraction of the total power capacity of the system, complex and therefore costly layouts should be avoided whenever possible.

In light of the above considerations, the recommendations given in previous works in the topic of ORC systems are partly followed here [12,13]. In particular:

- For the temperature range indicated in Table 2, the most interesting cycle configuration does not include superheating, and therefore dry saturated live vapour is expanded in the turbine.
- Even though a recuperator is advised for efficiency enhancement, this piece of equipment is not used in the proposed system for its negative effect on gas turbine waste heat recovery. This difference also arises when steam cycles of coal and combined cycle power plants are compared.

Relevant information of the cycle in Fig. 2 includes live vapour pressure/temperature, state 3′, and condenser pressure, state 4′, what in turn depends on heat source and sink temperatures, gas turbine exhaust gases and cooling medium respectively, and working fluid. The first set of boundary conditions is already defined by the fuel cell–gas turbine coupling and will not be discussed further in this section. For the selection of working fluid, previous works by the authors [14,15] provide the list in Table 3 where the following properties are included:

- Molar weight and critical temperature/pressure.
- Maximum pressure/temperature of the fluid: maximum live vapour pressure/temperature beyond which condensation will take place within the turbine. It is easily calculated by plotting a vertical line tangent to the steam-side of the saturation line in a T–s diagram, Fig. 2.
- Temperature stability limit: maximum temperature beyond which degradation of the working fluid is expected to take place.

Fig. 3 shows a temperature–entropy diagram of all the fluids considered (note that entropy scale has been adjusted so that condenser outlet, state 1′, is common to all fluids). It is important to note that only pure fluids and not mixtures have been considered in this work, Table 3, even though complex organic compounds like some siloxanes or others present very interesting features in waste heat recovery applications; among these properties, phase change at variable temperature is the most relevant [12]. These fluids are applied to the reference cycle in Figs. 2 and 3, assuming that the condenser temperature is the same for all cases, set up by a common heat sink like, for instance, available cooling water. Based on this common boundary conditions, the optimum results for each fluid are summarised in Table 4 where thermodynamic states at points 1′ to 4′ and global performance parameters, thermal/cycle efficiency $\eta_{th,ORC}$ and specific/useful work W_{sp}, are shown.

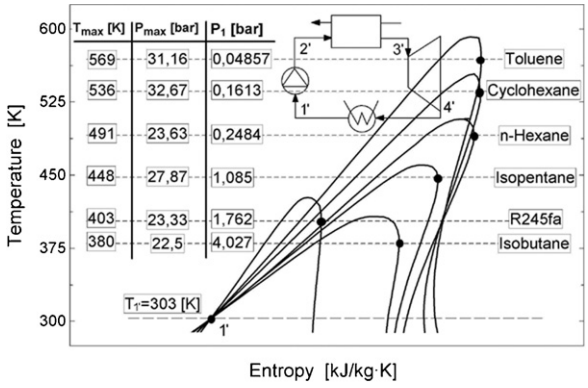

Fig. 3. T–s diagram of organic fluids under consideration.

$$\eta_{th,ORC} = \frac{(h_{3'} - h_{4'}) - (h_{2'} - h_{1'})}{h_{3'} - h_{2'}} \quad (2)$$

$$W_{sp} = W_t - W_p = (h_{3'} - h_{4'}) - (h_{2'} - h_{1'}) \quad (3)$$

Given the information in Table 4, it is concluded that using toluene yields the highest efficiency and useful work, even if cyclohexane performs similarly, while on the contrary isobutane performs rather inefficiently. Also worthy of note is the fact that some fluids condensate in vacuum conditions, toluene, cyclohexane and n-hexane, while others condensate at a pressure higher than atmospheric. This latter operating condition is advantageous with regard to non-condensable gases leaking into the system from the environment, as commented later.

Table 4
Reference ORC cycle analysis.

T (K)/p (bar)		1′	2′	3′	4′	$\eta_{th,ORC}$ (%)	W_{sp} (kJ kg^{-1})
Toluene	T	303	303.2	386.9	321.2	15.90	83.59
	p	0.049	1.137	1.114	0.050		
Cyclohexane	T	303	303.2	389.1	331.7	15.66	81.48
	p	0.161	2.666	2.613	0.165		
n-Hexane	T	303	303.2	390.5	343.2	14.84	76.61
	p	0.248	3.739	3.664	0.254		
Isopentane	T	303	303.6	400.3	341.7	15.34	76.40
	p	1.085	12.68	12.43	1.107		
R245fa	T	303	304.1	402.0	324.7	15.18	38.29
	p	1.762	23.36	22.89	1.798		
Isobutane	T	303	304.4	380.0	319.3	12.78	53.24
	p	4.027	22.96	22.50	4.110		

Table 5
Operating conditions of reference compound system.

MCFC	
Current density	1100 A m^{-2}
Active area	650 m^2
Fuel utilization	75%
Carbon utilization	60%
Temperature	923 K
Pressure	~1 bar
Gas turbine	
Pressure ratio	3:1
Turbine inlet temperature	903 K
Compressor/turbine efficiency	80/90%
Recuperator/HTHX effectiveness	85/80%
HRVG/ORC	
Minimum temperature difference	10 K
Condenser temperature	303 K

4. Integration of ORC subsystem into the compound system

The preliminary analysis developed in Section 3 is now expanded to system level, considering the reference layout in Fig. 1. The main assumptions incorporated in the model are:

- With regard to the fuel cell sub-model: lumped-volume approach based on the works by Iora and Campanari [16] and Koh et al. [17]. Details of the model are provided in Appendix A.
- With regard to the gas turbine sub-model: preliminary calculations performed for a 3:1 pressure ratio, typical of state of the art micro-turbines, which is later optimised along with live vapour pressure/temperature for maximum global efficiency of the compound system.
- With regard to the ORC sub-model: saturated live vapour, with live vapour temperature constrained by stability/condensation issues (i.e. lower than stability limit and maximum temperature according to Fig. 2). Recuperator not incorporated in order to enhance waste heat recovery.
- With regard to the heat recovery vapour generator HRVG: minimum temperature difference between hot and cold fluids set at 10 K, whether it is reached at the hot or cold end of the economiser.

A 500 kW atmospheric internal reforming MCFC with blower-driven gas recirculation from anode exhaust to cathode inlet, in order to meet a 60% carbon dioxide utilization, is considered, Fig. 1. Steam needed for the reforming process is generated at an auxiliary heat recovery boiler fed by fuel cell exhaust gases coming out from the fuel/air preheating section. With this layout, anodic gas recirculation is avoided, thus increasing energy availability for the gas turbine. This configuration and the operating conditions of the reference compound plant reported in Table 5 are then applied to systems running on each one of the organic fluids reported in Section 3. The results of such analysis are illustrated in Fig. 4.

According to Fig. 4, the impact of each organic fluid on system efficiency is quite the opposite to that reported in Section 3 for the stand alone ORC cycle. Hence, toluene and cyclohexane seem to yield the lowest global net efficiency, while R245fa credits an outstanding performance achieving one percentage point higher net global efficiency than the former fluids. The cause of this radical change is found in the behaviour of the heat recovery vapour generator HRVG, which is the component that matches gas turbine and ORC subsystems. Analytically, the contribution of the bottoming ORC system is expressed by a so-called bottoming cycle efficiency, η_{BC}, which can be further divided into the ability of the heat recovery vapour generator to recuperate waste heat from gas turbine exhaust gases and generate vapour, η_{HRVG}, and the thermal efficiency of the cycle that makes use of this vapour stream, $\eta_{th,\,ORC}$ as

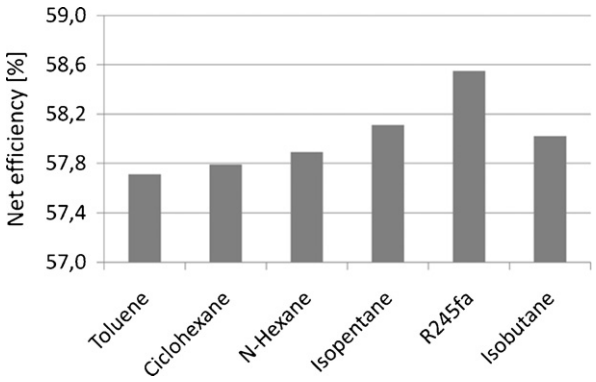

Fig. 4. Net efficiency of reference compound system in Fig. 1 with different organic fluids.

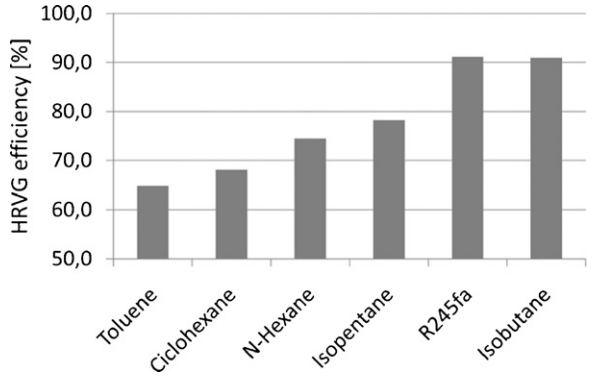

Fig. 5. Heat recovery vapour generator (HRVG) efficiency.

in Eq. (2)

$$\eta_{BC} = \eta_{HRVG} \cdot \eta_{th,ORC} \tag{4}$$

$$\eta_{HRVG} = \frac{\dot{m}_{ORC}(h_{3'} - h_{2'})}{\dot{m}_{GT}(h_{06} - h_{01})} \tag{5}$$

Fig. 5 illustrates the performance of the heat recovery vapour generator, η_{HRVG}, showing a great difference between the aforementioned fluids. Thus, the efficiency of this component drops dramatically when toluene or cyclohexane are used while it exceeds 90% for R245fa and isobutane, a difference of more than 25 percentage points emerging between the best and worst cases. For a better understanding of this remarkably different performance, the fundamental heat exchange T–Q diagrams have been plotted in Fig. 6 complying with the 10 K minimum temperature difference restriction indicated in Table 5. Three different cases are identified:

- Case 1: the minimum temperature difference is found at the cold end of the economiser. This is the case of isobutane.
- Case 2: the minimum temperature difference is found at the hot end of the economiser. This is the case of isopentane, toluene, cyclohexane and n-hexane.
- Case 3: T–Q lines for gas cooling and organic fluid heating are almost parallel in the economiser. Hence, the minimum temperature difference remains approximately constant at any point of this section of the HRVG. This is the case of R245fa.

The fundamental T–Q diagram of a heat recovery vapour/steam generator unit, and therefore the temperature profile as plotted in Fig. 6, is determined by the following parameters: hot gas inlet temperature, live vapour pressure/temperature and heat capacity of hot/cold fluids. Thus, Case 1 corresponds to systems where either hot gas inlet temperature and/or organic fluid heat capacity are very

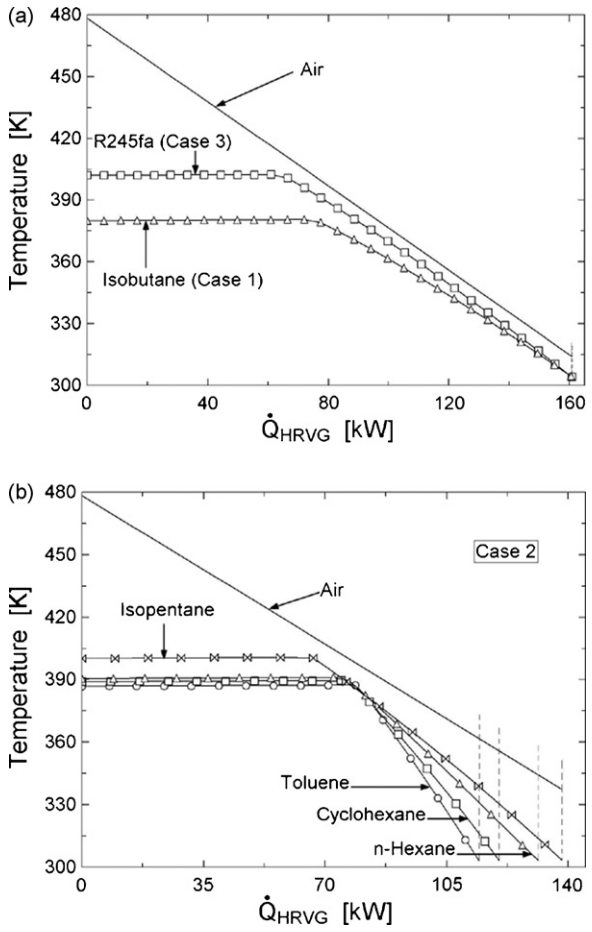

Fig. 6. Fundamental HRVG *T*–*Q* diagrams for different organic fluids.

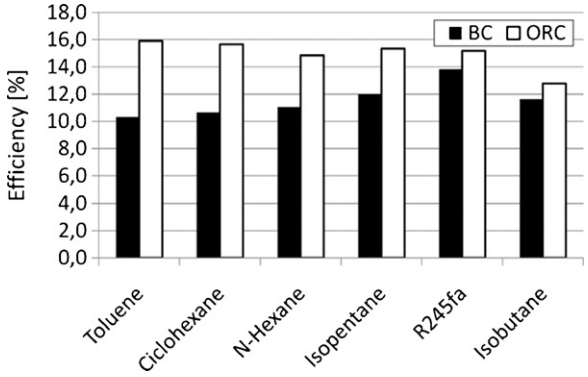

Fig. 7. Thermal and bottoming cycle efficiencies, Eq. (4).

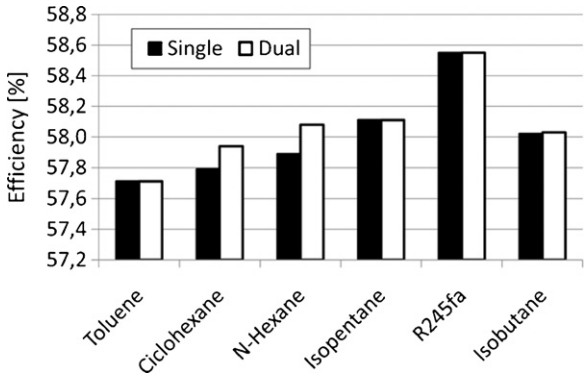

Fig. 8. Compound system efficiency for single and dual optimisation.

high and/or live steam temperature is low while Case 2 corresponds to the opposite operating conditions; case 3 lays in the middle and can be regarded as a transition case from Case 1 to Case 2.

Fig. 6 illustrates some very interesting aspects of HRVG heat transfer and explains the variable efficiency of this component when different organic fluids are considered. Hence, Fig. 6 shows that even though all organic fluids enter the HRVG at the same inlet temperature of 303 K, which is determined by the cooling medium, stack temperature differs from one another: toluene yields the highest value, around 360 K, and isobutene and R245fa the lowest, 315 K. This 45 K temperature difference implies that 28% less energy is recuperated from the exhaust gases if toluene is used, thus decreasing HRVG efficiency from around 90 to 65%.

The main root cause for the poor performance of toluene is its very high latent heat (359 kJ kg^{-1}) that is responsible for an important reduction of vapour mass flow rate. This low mass flow implies a steep increase of toluene temperature when heat is exchanged in the economiser and, therefore, a higher stack temperature. On the contrary, R245fa has a much lower latent heat (99.27 kJ kg^{-1}) and thus more vapour is generated at the HRVG. This brings about that more heat is recuperated in the economiser, reducing stack temperature and increasing efficiency.

From these considerations, it is concluded that the much better performance of the HRVG is able to compensate for a very poor and moderate ORC thermal efficiency in the cases of isobutane and R245fa respectively, as shown in Fig. 7.

In light of the results shown in Figs. 4–7, R245fa is selected as the working fluid for the ORC subsystem. The heat and mass balance of the reference system for the fuel cell/gas turbine operating conditions in Table 5 and the optimised R245fa Rankine cycle in Table 4 is shown in Table 6. A summary of the most relevant global performance parameters is also given in Table 7, showing that the ORC subsystem provides 5% additional power to the system which, accordingly, achieves 63.3/58.6 gross/net efficiency.

5. Simultaneous optimisation of gas turbine and Organic Rankine Cycle

So far, the analysis has concentrated on optimising the Organic Rankine Cycle for given fuel cell and gas turbine operating conditions but the potential benefits of a simultaneous optimisation of the entire bottoming system, including gas turbine and ORC, have not been explored. This option is now studied.

As already reported in the text, Table 2, there exists an optimum pressure ratio that yields the highest possible gas turbine efficiency for a given turbine inlet temperature. Hence, since this latter temperature depends essentially on the fuel cell operating temperature, which is assumed constant in the analysis, pressure ratio is the only parameter left to be optimised while live vapour pressure is the variable of choice for the ORC optimisation process. The aim of this multivariable optimisation process is to assess to what extent one subsystem is influenced by the other and find if this optimum design conditions are affordable for state of the art technology. At this point, it is worthy of note that even if the operating parameters reported in Table 4 are feasible for modern fuel cells [18] and gas turbines [19].

Fig. 8 shows a comparison between single (only ORC live vapour pressure) and dual (live vapour pressure and GT pressure ratio) optimisations. A very interesting aspect is that the optimised live vapour pressures obtained in each case are the same for isopentane, isobutane, R245fa and toluene while, on the contrary, some differences are detected for those fluids with intermediate perfor-

Table 6
Heat and mass balance of reference system working with R245fa.

State	T (K)	P (bar)	m (g s^{-1})	Molar fraction							
				HC	H_2	H_2O	CO	CO_2	O_2	N_2	R245fa
MCFC											
1	298	1	20.24	0.995	0	0	0	0	0	0.005	0
2	301.5	1.042	20.24	0.995	0	0	0	0	0	0.005	0
3	298	1.044	65.02	0	0	1	0	0	0	0	0
4	378.9	1.042	65.02	0	0	1	0	0	0	0	0
5	357.8	1.042	85.25	0.250	0	0.749	0	0	0	0.001	0
6	751.1	1.038	85.25	0.250	0	0.749	0	0	0	0.001	0
7	893	1.034	85.25	0.250	0	0.749	0	0	0	0.001	0
8	298	1	731.2	0	0	0	0	0.000	0.212	0.788	0
9	303	1.048	731.2	0	0	0	0	0.000	0.212	0.788	0
10	717	1.044	731.2	0	0	0	0	0.000	0.212	0.788	0
11	893	1.044	4161.6	0	0	0.168	0	0.035	0.114	0.683	0
12	923	1.024	3093.6	0	0.077	0.471	0.035	0.416	0	0.001	0
13	923	1.024	3937.5	0	0	0.174	0	0.011	0.106	0.709	0
14	982	1.016	4246.7	0	0	0.201	0	0.042	0.095	0.662	0
15	922.7	1.012	4246.7	0	0	0.201	0	0.042	0.095	0.662	0
16	922.7	1.012	3430.6	0	0	0.201	0	0.042	0.095	0.662	0
17	932.3	1.048	3430.6	0	0	0.201	0	0.042	0.095	0.662	0
18	925.3	1.044	3430.6	0	0	0.201	0	0.042	0.095	0.662	0
19	922.7	1.012	816.6	0	0	0.201	0	0.042	0.095	0.662	0
20	851.1	1.008	816.6	0	0	0.201	0	0.042	0.095	0.662	0
21	534.4	1.004	816.6	0	0	0.201	0	0.042	0.095	0.662	0
22	356.6	1	816.6	0	0	0.201	0	0.042	0.095	0.662	0
Cycle air GT											
01	298	1	1294.2	0	0	0	0	0.000	0.210	0.781	0
02	434.6	3	1294.2	0	0	0	0	0.000	0.210	0.781	0
03	671.5	2.94	1294.2	0	0	0	0	0.000	0.210	0.781	0
04	903	2.881	1294.2	0	0	0	0	0.000	0.210	0.781	0
05	713.4	1.041	1294.2	0	0	0	0	0.000	0.210	0.781	0
06	478.3	1.02	1294.2	0	0	0	0	0.000	0.210	0.781	0
07	314.1	1	1294.2	0	0	0	0	0.000	0.210	0.781	0
Cycle ORC											
1′	303	1.762	875	0	0	0	0	0	0	0	1
2′	304.1	23.36	875	0	0	0	0	0	0	0	1
3′	402	22.89	875	0	0	0	0	0	0	0	1
4′	324.7	1.798	875	0	0	0	0	0	0	0	1

mance. The analysis developed in the previous section is therefore updated with these newly optimised operating conditions of the GT-ORC coupling in order to check if any of these fluids can provide higher compound system efficiency. This information is illustrated in Figs. 8 and 9 where it is shown that, even if there is room for improvement when a dual optimisation is carried out for some organic fluids, R245fa is still the most efficient organic fluid as reported in Table 7.

Table 7
Performance of reference compound system MCFC–GT–ORC (R245fa).

System	Value
MCFC	
Gross power (kW)	500
Auxiliary power (kW)	46.2
Fuel mass flow (g s^{-1})	20.24
Gross efficiency (%)	50.9
Active area (m2)	650
GT	
Gross power (kW)	89.1
Gross efficiency (%)	27.9
Useful work (kJ kg^{-1})	70.8
BC	
ORC thermal efficiency (%)	15.2
Useful work (kJ kg^{-1})	38.3
HRVG efficiency (%)	91.2
Stack temperature (°C)	314.1
Bottoming cycle efficiency (%)	13.8
Global	
Gross power (kW)	621.6
Net power (%)	575.3
Gross efficiency (%)	63.3
Net efficiency (%)	58.6
MCFC power (%)	80.5
GT power (%)	14.3
Bottoming cycle power (%)	5.2

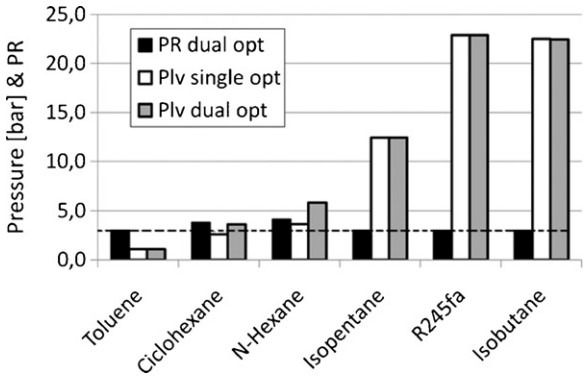

Fig. 9. Optimised variables for single and dual optimisation (dashed line shows assumed GT pressure ratio for single optimisation).

6. Additional considerations concerning organic fluids

The analysis shown in this work has focused on the thermodynamic properties of a number of organic fluids in order to determine which one of them yields the best compound system performance. To this aim, R245fa has been selected. Nevertheless, the analysis has not yet considered other properties of these fluids that are likely to

Table 8
Additional properties of organic fluids.

	$\rho_{3'}$ (kg m^{-3})	$\rho_{4'}$ (kg m^{-3})	T_{ign} (K)	LFL (%v)	UFL (%v)	NFPA
Toluene	3.34	0.17	695	1.1	7.1	3
Cyclohexane	7.37	0.51	518	1.3	8.4	3
n-Hexane	561.7	0.78	496	1.1	7.5	3
Isopentane	36.49	2.90	693	1.4	7.6	3
R245fa	149.9	9.41	–	–	–	0
Isobutane	66.98	9.91	693	1.8	8.4	4

be of interest from a practical point of view. Among others, hazard and compactness will be discussed in this section.

Table 8 shows relevant information concerning fluid density at turbine inlet and outlet sections, 3′ and 4′ in Fig. 1, calculated as per the operating conditions in Table 4. Interestingly, pressure and temperature that optimise bottoming cycle performance for the R245fa case also bring about the highest average density among all fluids since, even if n-hexane has a very high density at turbine inlet, the very low condensing pressure leads to a rather low density in this section of the cycle. Additionally, a complementary advantage of using R245fa is the higher than atmospheric condensing pressure that not only requires more compact equipments but also avoids that non-condensable gases leak into the system. Hence, compactness and ease of operation are additional beneficial features of the selected fluid.

Table 8 also collects very interesting data with regard to fluid flammability. Safety is a major concern when working with hydrocarbons (note that R245fa is also a hydrocarbon: pentafluoropropane) so it is mandatory to carry out an assessment about the hazard related to fluid selection as it might happen that the most efficient fluid not be recommendable for this type of applications. Thus, the following safety-related parameters are summarised in Table 8:

- Upper and lower flammability limits (LFL and UFL): richer and leaner composition (%v) of a fuel/air mixture that is flammable, should an ignition source be present.
- Autoignition temperature: temperature at which a fuel/air mixture will burn spontaneously, without an ignition source, as long as its composition lays within the flammability limits.
- NFPA flammability index: a measure of the flammability of a substance. It takes values from 0 (materials that will not burn) to 4 (will burn rapidly or completely vapourize at normal pressure and temperature, or is readily dispersed in air and will burn readily). It is assigned by the National Fire Protection Association NFPA in the United States [20].

According to Table 8, most of the organic fluids considered in this work are marked as very (3: liquids and solids that can be ignited under almost all ambient temperature conditions) or extremely (4) flammable except R245fa that is labelled as non-flammable. It is worth to note that, for instance, gasoline has the same NFPA mark (3) as most of the fluids in the comparison.

Hence, it is concluded that R245fa is extremely interesting from the point of view of safety due to its inert behaviour, what adds up to its thermodynamic features and to the fact that it is an HFC compound (hydrofluorocarbon) and therefore with zero ozone depletion potential.

7. Conclusions

The work presented in this article explores a novel combined power system based on high temperature fuel cell technology with the aim of increasing global efficiency up to or above 60%. Thus, a so-called compound system based on a conventional atmospheric molten carbonate fuel cell and hot air turbine hybrid system which incorporates a secondary bottoming system using Organic Rankine Cycle technology is proposed. This additional ORC system is embodied in the global system in a cascaded configuration.

With regard to the Organic Rankine Cycle, the main conclusion drawn from the analysis is that the heat recovery vapour generator plays a fundamental role. Thus, the organic fluid of choice is R245fa due to its superb performance at the HRVG even if ORC thermal efficiency is lower than with other fluids.

With regard to the compound system, the main conclusions are:

1. System efficiency reaches and even exceeds 60%, depending on the particular operating conditions, therefore accomplishing one of the objectives stated initially.
2. System efficiency is 5 percentage points higher than conventional MCFC-GT hybrid systems based on atmospheric molten carbonate fuel cells.
3. Simultaneous optimisation of gas turbine and ORC does not improve the performance of the compound system with respect to using usual settings of already existing MCFC-GT.
4. For those fluids to which the previous statement does not apply, the resulting optimum gas turbine pressure ratio is still within the feasible operating range of state of the art technology.
5. The selected organic fluid, R24fa, provides additional advantages like non-flammability or higher than atmospheric condenser pressure.

In summary, a fuel cell based system able to achieve 60% efficiency has been developed, even though conservative modelling assumptions were considered. This system adds complexity to the already complex state of the art hybrid systems but confirms that fully exploiting the concept of thermal integration can improve the performance of these conventional hybrids (5 percentage points or 10% relative increase in the case studied). Future work will explore part load performance of the system in order to confirm its high efficiency under these operating conditions and to detect potential thermal mismatches brought about by its complex configuration.

Appendix A.

The works by Iora and Campanari [16], for the general model configuration, and Koh et al. [17], for the calculation of voltage losses, are used to construct a lumped-volume model of performance of molten carbonate fuel cells.

The fuel cell is fed by a mixture of hydrocarbons, i.e. natural gas of variable composition, and steam generated at an external heat recovery steam generator that recuperates waste energy at system exhaust, Fig. 1. The amount of steam added to the raw fuel is set by the commonly used Steam To Carbon Ratio *STCR*:

$$STCR = \frac{\eta_{H_2O}}{\eta_{CH_4} + \eta_{CO}} \quad (A.1)$$

This fuel-steam mixture is indirectly reformed within the fuel cell, thus exploiting the heat released by hydrogen oxidation with

a twofold purpose of (i) cooling down the stack and (ii) saving primary energy for the reforming process. A universal steam reforming reaction for oxygen-free compounds is considered [7,21]:

$$C_\alpha H_\beta + \alpha \cdot H_2O \rightarrow \alpha \cdot CO + \left(\alpha + \frac{\beta}{2}\right) \cdot H_2 \quad (A.2)$$

Eq. (A.2) is further simplified in this work where only methane (CH_4), ethane (C_2H_6), propane (C_3H_8) and butane (C_4H_{10}) are considered, inasmuch as $\beta = 2\cdot(\alpha + 1)$ for these compounds. Hence:

$$C_\alpha H_{2(\alpha+1)} + \alpha \cdot H_2O \rightarrow \alpha \cdot CO + (2\alpha + 1) \cdot H_2 \quad (A.3)$$

This reaction develops completely at the reforming section of the cell while, on the contrary, water–gas shift, Eq. (A.4) is assumed to reach equilibrium at cell operating temperature; the equilibrium constant depends on temperature as shown in Eq. (A.5) [22]:

$$CO + H_2O \rightarrow CO_2 + H_2 \quad (A.4)$$

$$\log K_{shift} = 5.47 \times 10^{-12} T^4 - 2.5748 \times 10^{-8} T^3 + 4.6374 \times 10^{-5} T^2 - 3.9150 \times 10^{-2} T + 13.2097 \quad (A.5)$$

Based on the previous considerations, fuel flow rate depends on cell current density, through Faraday's law, and fuel utilization. Globally, fuel flow rate n_{fuel} is evaluated as:

$$\eta_{H_2,reac} = \frac{j \cdot A}{2F} \quad (A.6)$$

$$U_f = \frac{(j \cdot A)/(2F)}{n_{shift} + \sum_{\alpha=1}^{4} (2\alpha + 1) x_{C_\alpha H_{2(\alpha+1)}} \cdot n_{fuel}} \quad (A.7)$$

where $x_{C_\alpha H_{2(\alpha+1)}}$ stands for the molar fraction of $C_\alpha H_{2(\alpha+1)}$ in the fuel and x_{shift} is the molar rate of reaction corresponding to water–gas shift, Eq. (A.4). Air mass flow is obtained from a global heat balance equation applied to a control volume around the fuel cell stack, including the internal reformer. Hence, conservation of energy imposes that gas temperature/enthalpy increase from inlet to outlet, left term in Eq. (A.8), is due to heat released by reforming, oxidisation and water–gas shift reactions, right term in Eq. (A.8):

$$\sum_{an,ca} n_{out} \cdot h_{m,out} - \sum_{an,ca} n_{in} \cdot h_{m,in} = -\sum n_r \cdot h_{m,r} \quad (A.8)$$

It is worth noting that the cathode is fed by a mixture of air and CO_2 rich gas by-passed from the catalytic burner located at cell exhaust where excess fuel is burnt. Carbon dioxide recirculation is necessary to prevent carbonate starvation in the electrolyte due to hydrogen oxidation at the anodic interface, Eq. (A.9). The fraction of gases that is recirculated is calculated with the following carbon utilization factor U_{CO_2}, Eq. (A.11).

$$H_2 + CO_3^{=} \rightarrow H_2O + CO_2 + 2e^- \quad (A.9)$$

$$O_2 + CO_2 + 2e^- \rightarrow CO_3^{=} \quad (A.10)$$

$$U_{CO_2} = \frac{n_{CO_2,reac}}{n_{CO_2 inlet}} \quad (A.11)$$

The operating voltage of the cell V depends on materials, fuel/oxidant compositions, pressure and temperature essentially. It is calculated with the following set of equations:

$$V = E - j \cdot R_{tot} = E - j \cdot (R_{ohm} + R_{an} + R_{ca}) \quad (A.12)$$

$$E = E_0 + \frac{RT}{2F} \ln\left(\frac{p_{H_2,an} \cdot p_{O_2,ca}^{1/2}}{p_{H_2O,an}}\right) + \frac{RT}{2F} \ln\left(\frac{p_{CO_2,ca}}{p_{CO_2,an}}\right) \quad (A.13)$$

$$R_{ohm} = 0.5 \times 10^{-4} \exp\left(3016\left(\frac{1}{T} - \frac{1}{923}\right)\right) \quad (A.14)$$

$$R_{an} = 2.27 \times 10^{-9} \exp\left(\frac{6435}{T}\right) p_{H_2,an}^{-0.42} p_{CO_2,an}^{-0.17} p_{H_2O,an}^{-1.0} \quad (A.15)$$

$$R_{ca} = 7.505 \times 10^{-10} \exp\left(\frac{9298}{T}\right) p_{O_2,ca}^{-0.43} p_{CO_2,ca}^{-0.09} \quad (A.16)$$

where E and E_0 are the actual and standard Nernst voltage. R_{ohm} stands for the voltage drop due to the internal resistance to the flow of charge, whether electrons or ions, in the components of the fuel cell stack while R_{an} and R_{ca} are known as polarisation losses which depend on the concentration of chemical species involved in the oxidation/reduction reactions at each electrode. All these resistances are expressed in ($\Omega\,m^2$). Finally, it is interesting to note that E is calculated as the mean value between inlet and outlet of the cell so as to account for the variable composition of fuel and oxidant through the stack.

From Eqs. (A.1)–(A.16), the electric power produced by the fuel cell stack is calculated as:

$$\dot{W}_{el} = j \cdot V \cdot A_{cell} \quad (A.17)$$

References

[1] A.F. Massardo, F. Lubelli, J. Eng. Gas Turb. Power-Trans. ASME 122 (2000) 27–35.
[2] R.A. Roberts, J. Brouwer, E. Liese, R.S. Gemmen, J. Eng. Gas Turb. Power-Trans. ASME 128 (2006) 294–301.
[3] M.L. Ferrari, E. Liese, D. Tucker, L. Lawson, A. Traverso, A.F. Massardo, J. Eng. Gas Turb. Power-Trans. ASME 129 (2007) 1012–1019.
[4] S.E. Veyo, L.A. Shockling, J.T. Dederer, J.E. Gillet, W.L. Lundberg, J. Eng. Gas Turb. Power-Trans. ASME 124 (2002) 845–849.
[5] M.B. Landau, U.S. Patent 3,976,506 (1976).
[6] D.J. White, Proceedings of the International Gas Turbine & Aeroengine Congress and Exhibition Indianapolis, 1999.
[7] S. McPhail, A. Moreno, R. Bove, International Status of Molten Carbonate Fuel Cell (MCFC) Technology, ENEA Report RSE/2009/181, 2008.
[8] T.C. Hung, T.Y. Shai, S.K. Wang, Energy 22 (1997) 661–667.
[9] T.C. Hung, Energy Convers. Manage. 42 (2001) 539–553.
[10] P.J. Mago, L.M. Chamra, C. Somayaji, Proc. Inst. Mech. Eng. Part A: J. Power Energy 221 (2007) 255–264.
[11] H.I.H. Saravanamuttoo, G.F.C. Rogers, H. Cohen, P.V. Straznicky, Gas Turbine Theory, vol. 6, Pearson, Harlow, 2009.
[12] G. Angelino, P. di Paliano, Energy 23 (1998) 449–463.
[13] G. Angelino, M. Gaia, E. Macchi, Proceedings of the International VDI-Seminar, Zürich, September, 1984, pp. 465–482.
[14] R. Chacartegui, D. Sánchez, J.M. Muñoz, T. Sánchez, Appl. Energy 86 (2009) 2162–2170.
[15] D. Sánchez, R. Chacartegui, A. Muñoz, T. Sánchez, Proceedings of EFC2009 Third European Fuel Cell Technology & Applications Conference, Rome, 2009.
[16] P. Iora, S. Campanari, J. Fuel Cell Sci. Technol. 4 (2007) 501–510.
[17] J. Koh, H. Seo, Y. Yoo, H.C. Lim, Chem. Eng. J. 87 (2002) 367–379.
[18] J.R. Selman, Proceedings of the Molten Carbonate Fuel Cells (MCFC) and Phosphoric Acid Fuel Cells (PAFC) Workshop, Palm Springs, CA, 2009.
[19] C. Soares, Microturbines, Buterworth-Heinemann, Burlington, 2007.
[20] National Fire Protection Association website www.nfpa.org.
[21] B. Viswanathan, M. Aulice Scibioh, Fuel Cells: Principles and Applications, Universities Press, Hyderabad, 2007.
[22] U.G. Bossel, Final Report on SOFC Data Facts and Figures, Swiss Federal Office of Energy, Berne, 1992.